BBA 4019

STUDIES OF THE KINETICS OF AMINO ACID TRANSPORT, INCORPORATION INTO PROTEIN AND OXIDATION IN KIDNEY-CORTEX SLICES

LEON E. ROSENBERG, MONES BERMAN AND STANTON SEGAL

Metabolism Service, National Cancer Institute, Office of Mathematical Research and Clinical Endocrinology Branch, National Institute of Arthritis and Metabolic Diseases, National Institutes of Health, Bethesda, Md. (U.S.A.)

(Received September 10th, 1962)

SUMMARY

The present report describes an approach to the study of the steady-state kinetics of amino acid transport and protein synthesis in rat-kidney-cortex slices, using multi-compartment models. The following conclusions seem justified from the data presented:

1. Using inulin and the non-metabolizable amino acid, α-aminoisobutyric acid, amino acid uptake could be characterized by a three-compartment "parallel" model representing the medium, extracellular space and intracellular space. Appropriate influx and efflux rate constants were calculated.

2. 2,4-Dinitrophenol and incubation at 27° significantly effected the rate of efflux of α-aminoisobutyric acid from the intracellular space, as well as the rate of influx, suggesting that efflux phenomena are metabolically linked.

3. Kinetic studies of combined transport and protein synthesis with glycine and L-lysine indicated that equilibration of exogenous amino acid with the intracellular pool need not occur before incorporation into protein takes place.

4. The kinetics of $^{14}CO_2$ evolution from labeled L-lysine indicated that the rate of amino acid oxidation reflected the buildup of the intracellular lysine pool.

5. The results suggest that the mathematical approach, used in the analysis of the experimental data, provides means of quantitating and understanding membrane phenomena and the relationship between rates of membrane transfer and subsequent intracellular utilization.

INTRODUCTION

Although the molecular nature of amino acid transport, intracellular-pool formation and accumulation against chemical gradients remains obscure, the kinetics of these phenomena have been extensively studied *in vitro* in several single-cell systems, including bacteria[1,2], ascites-tumor cells[3-5], yeast[6,7] and mammalian lymphocytes[8]. In contrast to the large body of knowledge in single-cell systems, very little information has been presented on kinetic aspects of amino acid transport or intracellular utili-

zation in organized mammalian tissues. KIPNIS *et al.*[8], working with isolated intact rat diaphragm, corroborated earlier observations in single-cell systems which have suggested that the intracellular amino acid pool is not a single homogeneous compartment. More recently AKEDO AND CHRISTENSEN[9], using the same tissue preparation, described the mode of action of insulin on the uptake of the non-metabolizable amino acid, α-aminoisobutyric acid.

Previous studies from this laboratory have shown that rat-kidney-cortex slices accumulate a variety of α-amino acids against chemical gradients *in vitro*[10,11]. This concentrative transfer is dependent on aerobic metabolism and is markedly altered by changes in temperature of incubation, or the presence of a variety of substances including other amino acids[11], 2,4-dinitrophenol[10], phlorizin[12] and maleic acid[13].

The present studies, utilizing the multi-compartment model approach of BERMAN *et al.*[14,15], were undertaken to estimate rates of amino acid influx into and efflux from the slice cells, to relate the rates of cellular accumulation with those of subsequent incorporation into protein and oxidation to CO_2, and to define the mode of action of some of the agents noted above on the phenomena under investigation. The present report describes in detail the methods used in the collection, analysis and interpretation of data, and summarizes our findings with α-aminoisobutyric acid, glycine and L-lysine.

EXPERIMENTAL PROCEDURE

Materials

α-[1-^{14}C]Aminoisobutyric acid (spec. act. 3.39 mC/mmole) was obtained from Isotope Specialties Company. [2-^{14}C]Glycine (spec. act. 1.19 mC/mmole), L-[^{14}C]-lysine (spec. act. 1.62 mC/mmole) and [*carboxy*-^{14}C]inulin (spec. act. 1.0 mC/mmole) were obtained from the Volk Radiochemical Company. Each of the labeled amino acids was chromatographically pure in single-dimension ascending paper-chromatographic studies using butanol – acetic acid – water (4:1:2, v/v). Unlabeled L-lysine and glycine were purchased from Nutritional Biochemicals Company, and unlabeled α-aminoisobutyric acid was obtained from The Mann Research Laboratories. The 2,4-dinitrophenol was obtained from The Eastman Chemical Company.

Methods

Male Sprague–Dawley rats, weighing from 140 to 180 g were used in all experiments, and were fed a Purina(R) rat chow diet and water *ad libitum* until sacrificed by stunning and decapitation. The techniques employed for the preparation of kidney-cortex slices, pre-incubation in Krebs–Ringer bicarbonate buffer (pH 7.4) at room temperature, estimation of total tissue water, determination of extracellular space with [^{14}C]inulin and assessment of intracellular and medium concentration of amino acid have been described in detail previously[10,16]. In the present experiments, steady-state conditions were used throughout and were achieved as follows: Groups of slices were incubated aerobically at 37° in 25 ml Erlenmeyer flasks containing 2.0 ml of Krebs–Ringer bicarbonate buffer (pH 7.4) plus unlabeled amino acid, until the intracellular amino acid concentration approached equilibrium (60–90 min)[10,11]; the slices were then transferred to flasks prepared in exactly the same way, except for the substitution of an equivalent concentration of ^{14}C-labeled amino acid, regassed and incubated for periods ranging from 5 to 120 min. Each flask contained

three cortex slices, totalling 80–120 mg in weight. Following incubation, which was terminated by removing the slices from the medium, the tissues were prepared for analysis. The medium concentrations used for α-aminoisobutyric acid, glycine and lysine were 0.065, 0.170 and 0.060 mM respectively. These concentrations were chosen because they represented values far below the K_m for each amino acid[10,11].

If amino acid uptake alone was being investigated (as with α-aminoisobutyric acid), the free intracellular amino acid pool was extracted with boiling distilled water, and the radioactivity of the aqueous extract and remaining medium assessed as described previously[10] using an automatic liquid scintillation spectrometer with an efficiency of 57 % for the system used. Aliquots of the aqueous tissue extracts were chromatographed using the single-dimension system mentioned above, and, with appropriate counting techniques[10], greater than 90 % of the recovered tissue radioactivity was uniformly found with the appropriate R_F for the specific amino acid studied.

When intracellular accumulation and incorporation into tissue protein were investigated jointly, the slices were homogenized in 10.0 ml of cold 10 % trichloroacetic acid using a motor-driven Potter–Elvehjem homogenizer. The homogenates were then poured into centrifugation tubes, spun for 5 min at 800 × *g*, and the supernatant decanted. Aliquots of the trichloroacetic acid supernatant and medium were prepared for counting exactly as described for the aqueous tissue extract, and gave comparable results. The trichloroacetic acid precipitable tissue proteins were resuspended and prepared by the method of STEINBERG *et al.*[17], as modified by MANCHESTER AND YOUNG[18]. The specific radioactivity of the proteins was determined by the method of STEINBERG *et al.*[17] in an automatic liquid scintillation spectrometer with an efficiency of 44 % for the system used.

The rate of $^{14}CO_2$ evolution from slices incubated with uniformly labeled L-[^{14}C]-lysine under steady-state conditions was determined by collecting the evolved CO_2 and counting it according to previously described techniques[19].

Data analysis

The radioactivity per ml of medium was expressed as a fraction of the initial medium radioactivity. The radioisotope data for the tissues were expressed as a fraction of the initial medium radioactivity per 100 mg tissue (or tissue equivalent), and thus contained radioactivity in the extra- and intracellular spaces of the slice. These data were fitted to models proposed on the basis of the experimental values and the architecture of the tissue slice. The models consisted of a number of compartments with transition probabilities (or turnover rates) between them. Least squares fitting of the data to the models was obtained using digital computer techniques described by BERMAN *et al.*[14,15], which yielded values for the transition probabilities and estimates for their standard deviations. In deriving these values, the data from the kinetics of uptake of inulin and amino acids were used together to resolve the intra- and extracellular space rate constants.

In the figures used to represent models, the compartments are indicated by open circles, and the unidirectional rate constants by arrows between the compartments. The rate constants, designated by the latter λ are expressed in min^{-1}. The site of introduction of labeled substrate is shown by a vertical arrow with an asterisk.

RESULTS

Extracellular space analysis

Previous results from this laboratory indicated that the space of distribution of [^{14}C]inulin provided an accurate estimation of the extracellular volume in kidney slices[16]. In Fig. 1, the medium disappearance and the tissue uptake of [^{14}C]inulin are plotted against duration of incubation. As shown by the agreement betwe n the observed and calculated values, a good least-squares fit was obtained with the two-compartment model shown (Fig. 1). Under steady-state conditions the movement of inulin between these two compartments may be expressed by the following equation:

$$\lambda_{EM} C_M = \lambda_{ME} C_E \qquad (1)$$

where λ_{EM} represents the fractional rate of movement into the extracellular space from the medium, λ_{ME} represents the fractional rate of flow in the reverse direction, and C_M and C_E represent the sizes of the medium and extracellular compartments respectively, expressed in ml or mmoles. Substituting calculated values for λ_{ME} and λ_{EM} from Fig. 1, Eqn. 1 can be rearranged to yield:

$$\frac{C_M}{C_E} = \frac{0.211}{0.0025} = 84.4 \qquad (2)$$

Eqn. 2 indicates that the calculated ratio of compartment sizes between the medium and extracellular space is approx. 84:1. This value agrees very well with the value of 81:1 determined directly using total tissue-water content, medium volume, and inulin space[16].

Throughout the remainder of the analysis, it is assumed that the amino acids studied equilibrate with the extracellular component of the slice in a fashion identical to that of inulin, and that the concentration of amino acid in the extracellular space is equal to that in the medium. This assumption seems justified by the data obtained when extracellular distribution in the kidney slice was measured with sucrose, whose molecular weight more closely approaches that of the amino acids studied. When cellular penetration of sucrose was prevented with phlorizin[16], the kinetics of sucrose distribution were virtually identical with those of inulin.

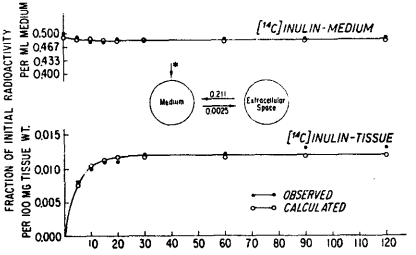

Fig. 1. Tissue uptake and medium disappearance of [^{14}C]inulin. The insert defines a two-compartment model postulated from the observed data. The starred arrow indicates site of introduction of labeled substrate, and the numerical values associated with the unidirectional arrows represent the turnover rate constants between the two compartments.

Kinetics of α-aminoisobutyric acid uptake

Initially, a 3-compartment "series" model (Fig. 2, insert) was postulated to describe the movement of α-aminoisobutyric acid in the kidney slice. However, as shown by the curves comparing tissue uptake of α-[1-^{14}C]aminoisobutyric acid and [^{14}C]inulin (Fig. 2), a satisfactory solution was not obtained because the initial rate of α-aminoisobutyric acid uptake far exceeded that for inulin (as shown by the 5-min points). This result indicated that the rate of influx of the amino acid into the intracellular compartment was too rapid to be explained by postulating that all amino acid molecules must traverse the extracellular space before entering the cellular compartment, and that a more direct pathway between the medium and the intracellular space must exist. In fact, a "parallel" model that permits molecules to move simultaneously into the extra- and intracellular spaces from the medium fitted the data well, as shown in Fig. 3, in which tissue uptake and medium disappearance for α-aminoisobutyric acid are plotted. Values for the rate constants that describe the bidirectional movement of amino acid between the medium and the intracellular space (λ_{MI} and λ_{IM}) and between the medium and the extracellular space (λ_{ME} and λ_{EM}) were calculated. In the latter case, the values were set equal to those obtained with inulin.

The parallel model is not the only 3-compartment model that fits the data, and other models were also tested. As noted in Fig. 4A, a model postulating unidirectional flow from the medium into the intracellular space, and from the intracellular to the

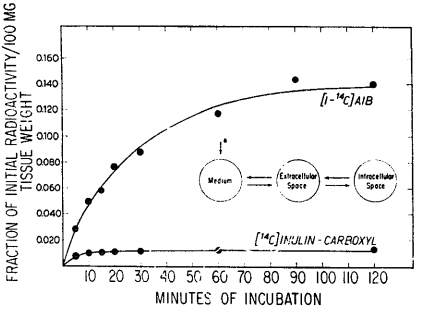

Fig. 2. Tissue uptake of [^{14}C]inulin and α-[1-^{14}C]aminoisobutyric acid (AIB). As discussed in the text, the rapidity with which α-aminoisobutyric acid molecules enter the slice indicates that the threecompartment series model (shown in insert) is incompatible with the observed results.

extracellular compartments yielded a satisfactory solution, with rate constant estimates which closely approximated those noted in Fig. 3. As will be discussed subsequently, this model is of interest in that the direction of amino acid movement simulates the pathway utilized during renal tubular reabsorption. The addition of bidirectional pathways between compartments 2 and 3 (Figs. 4B and 4C) resulted in non-unique solutions, meaning that many sets of values could fit the data equally well. The available data did not permit a unique choice between the various models, and each is theoretically possible.

In studies to be presented subsequently, the model shown in Fig. 3, was selected for convenience, but it should be noted that virtually identical results were also obtained with the model shown in Fig. 4A.

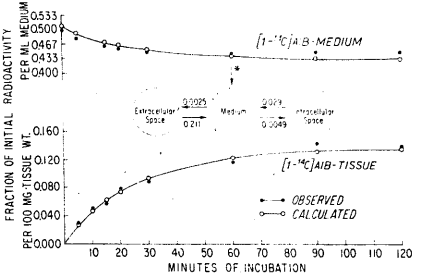

Fig. 3. Tissue uptake and medium disappearance of α-[1-^{14}C]aminoisobutyric acid (AIB). As shown by the agreement between calculated and observed values, the three-compartment "parallel" model shown is consistent with the experimental observations. The medium α-aminoisobutyric acid concentration was 0.065 mM, and the data points represent the mean of triplicate determinations.

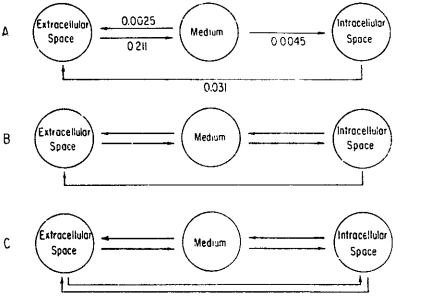

Fig. 4. Other models postulated to define kinetics of α-aminoisobutyric acid uptake. A, Compatible model indicating unidirectional movement from medium to intracellular and from intracellular to extracellular species. B and C, Models which yielded non-unique solutions.

Effect of dinitrophenol and temperature reduction on kinetics of α-aminoisobutyric acid uptake

Previous results from this laboratory showed that 2,4-dinitrophenol and reduction of incubation bath temperature from 37° to 27° both resulted in distinct decreases in the intracellular α-aminoisobutyric acid concentration after 90-min incubations[10]. Steady-state incubation studies under these altered conditions were, therefore, carried out to determine the mode of action of these altered conditions on transfer mechanisms in the kidney slice and to test the model selected. The tissue

TABLE I

EFFECT OF 2,4-DINITROPHENOL AND TEMPERATURE REDUCTION ON KINETICS OF α-AMINOISOBUTYRIC ACID TRANSPORT IN KIDNEY-CORTEX SLICES

Experimental conditions	Compartment size (μmoles)*		Fractional turnover rates** (min⁻¹)		Difference from control (%)		Net flux (μmoles/min)	Equilibrium distribution ratio***
	Medium	Intracellular space	λ_{IM}	λ_{MI}	λ_{IM}	λ_{MI}		
Control	0.130	0.022	0.0049 ± 0.0002	0.0290 ± 0.0020			0.0064	5.9
2,4-Dinitrophenol ($5 \cdot 10^{-5}$ M)	0.130	0.014	0.0036 ± 0.0004	0.0336 ± 0.0055	−27	+16	0.0047	4.3
Incubation at 27°	0.130	0.021	0.0016 ± 0.0001	0.0107 ± 0.0013	−67	−63	0.0021	5.8

* Compartment sizes calculated as in Eqn. 1: $\lambda_{IM}C_M = \lambda_{MI}C_I$, where: λ_{IM} = rate constant for movement into intracellular space from medium; λ_{MI} = rateconstant for movement into medium from extracellular space; C_M = medium compartment size (μmoles); C_I = intracellular compartment size (μmoles).

** Expressed as turnover rate ± standard deviation.

*** Defined as $\frac{\text{intracellular concentration (}\mu\text{moles/ml)}}{\text{medium concentration (}\mu\text{moles/ml)}}$

TABLE II

KINETICS OF GLYCINE AND L-LYSINE TRANSPORT AND INTRACELLULAR UTILIZATION IN KIDNEY SLICES

Amino acid	Medium concentration (μmoles/ml)	Fractional turnover rates* (min⁻¹)				Net flux into (mμmoles/min)		
		λ_{IM}	λ_{MI}	λ_{PM}**	λ_{CI}***	Intracellular pool	Protein	CO_2
[2-^{14}C]Glycine	0.170	0.0073	0.0429	0.00010		2.480	0.034	
		±0.0006	±0.0058	±0.00002				
Uniformly labeled L-[^{14}C]lysine	0.060	0.0057	0.0840	0.00030	0.0140	0.684	0.036	0.114
		±0.0003	±0.0089	±0.000009	±0.0006			

* Values represent calculated turnover rate ± standard deviation.

** λ_{PM} = rate of incorporation of amino acid into trichloroacetic acid-precipitable protein from medium.

*** λ_{CI} = rate of evolution of $^{14}CO_2$ from intracellular amino acid pool.

uptake curves for α-aminoisobutyric acid under these conditions are shown in Fig. 5, and the calculated rate constants, compartment sizes, net fluxes and distribution ratios derived from these curves are presented in Table I. The 2,4-dinitrophenol exerted its inhibitory effect on tissue uptake by retarding influx and accelerating efflux of α-aminoisobutyric acid from the kidney slice. In contrast, incubation at 27° produced no final difference in the equilibrium tissue content as shown by the 180-min value in Fig. 5, but a significantly longer duration of incubation was required to achieve equilibrium than with tissues incubated at 37°. Analysis of these data (Table I) indicated an essentially equal reduction in influx rate and efflux rate at the reduced temperature.

Combined kinetics of glycine uptake and incorporation into protein

Using [2-^{14}C]glycine, it was possible to follow simultaneously the rates of intracellular accumulation and incorporation into labeled trichloroacetic acid-precipitable

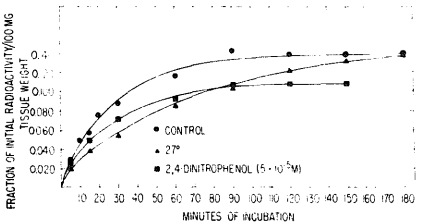

Fig. 5. Effect of 2,4-dinitrophenol and reduction of incubation temperature to 27° on tissue uptake of α-aminoisobutyric acid. When incubation duration at 27° was extended to 210 min, tissue uptake was equivalent to that shown at 180 min, indicating that equilibrium had been achieved. The calculated changes in the fractional rate constants and compartment sizes are shown in Table I.

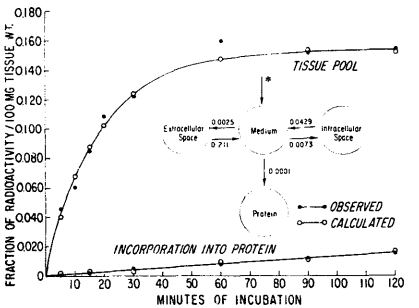

Fig. 6. Curves of [2-^{14}C]glycine uptake and incorporation into slice protein. The medium glycine concentration was 0.17 mM. As discussed in the text, the four-compartment model shown yielded a satisfactory solution to the experimental observations. The data points represent the mean of triplicate determinations.

tissue protein. As shown in Fig. 6, the uptake curve was exponential while the rate of incorporation into protein was constant throughout the incubation interval studied. As discussed previously by other workers[7,8], if the availability of precursor amino acid had been dependent on equilibration with the total intracellular amino acid pool,

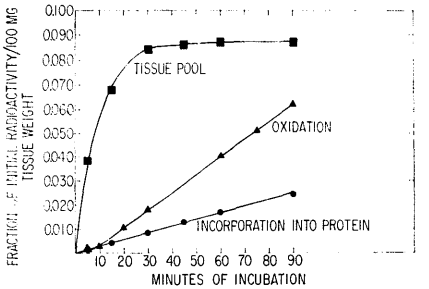

Fig. 7. Curves of uniformly labeled L-[^{14}C]lysine uptake, oxidation and incorporation into protein. The medium lysine concentration was 0.060 mM. In contrast to the incorporation data, the oxidation curve reflected the intracellular lysine accumulation. The data points represent the mean of triplicate determinations.

an early lag in the incorporation curve should have been noted. It was, therefore, apparent that the pathway to a "protein-synthesizing pool" in the analytical model could not originate from the total intracellular amino acid pool. In fact, the linear rise in protein specific activity suggested that operationally it could be supplied from the medium directly. Because of this, the protein pool was arbitrarily appended to the medium (Fig. 6) with the understanding that present knowledge cannot distinguish between several possibilities, including incorporation of the labeled amino acid directly into membrane protein, amino acid activation in or adjacent to the

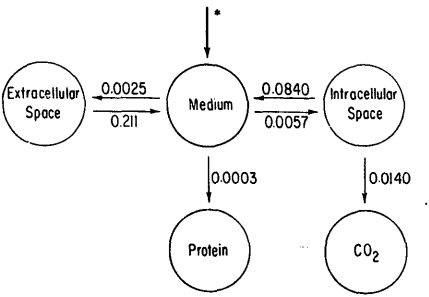

Fig. 8. Five-compartment model which yielded a satisfactory least-squares fit to the data shown in Fig. 7.

cell membrane, and the existence of a rapidly turning-over protein precursor pool within the intracellular compartment.

With this operational model, a satisfactory least-squares fit of the data was achieved, and appropriate turnover rates calculated (Fig. 6). The uncertainty of the turnover rates is indicated (Table II) by the magnitude of their standard deviations. The fractional rate of incorporation into protein was about 1/70 that of the rate of influx of amino acid into the cellular pool, as shown by the calculated flux values in Table II.

Kinetics of uptake, protein synthesis and amino acid oxidation with L-*lysine*

In contrast to labeled glycine from which negligible quantities of $^{14}CO_2$ were evolved during 120-min incubation studies, uniformly labeled L-[^{14}C]lysine was readily oxidized to $^{14}CO_2$, thus providing an additional parameter of intracellular utilization which could be followed under steady-state conditions. As seen in Fig. 7, the curves of L-lysine appearance in the tissue pool and incorporation into protein were similar to those observed with glycine. The evolution of $^{14}CO_2$, however, followed a curvilinear plot with a definite early lag. It was, therefore, assumed that the rate of CO_2 production depended on the concentration of free intracellular amino acid, and a model for lysine was constructed with an additional "amino acid oxidation pool" as shown in Fig. 8. With this model, a satisfactory least-squares fit was obtained, and rate constants calculated (Fig. 8). As noted in Table II, the fractional rate of incorporation into protein was small when compared to either the rate of amino acid influx into the cellular pool or the rate of amino acid oxidation.

DISCUSSION

Physical-mathematical models have been used to attack a wide variety of biological problems in recent years[15,20], but such models have been utilized only rarely to study the kinetics of transport and intracellular utilization of amino acids[6-8]. In the present studies, models of minimal complexity to explain the experimental observations have been constructed, with the understanding that such treatment may well represent a distinct over-simplification of the true biological phenomena investigated. It must be emphasized that such expressions as "the extracellular space" or "the intracellular space" represent operational designations only, and may have to be modified or summarily discarded in the light of future evidence.

A great majority of the cells in the kidney-cortex slice are in direct contact with the incubation medium because of their arrangement around tubular lumena. Furthermore, the lumenal margin of the tubular cells is composed of a "brush border" made up of countless micro-villi. This unique histologic configuration which presents a vast surface for direct cellular penetration, very likely explains the relative unimportance of the extracellular space as a barrier to cell entry, as evidenced by the failure of a "series" model (Fig. 2) to yield a satisfactory solution to the kinetics of amino acid uptake.

It is of interest that one of the models prepared in the present study (Fig. 4A) bears distinct resemblance to the present concept of substrate movement during renal tubular reabsorption. The unidirectional passage of material directly into the intracellular compartment from the medium can be visualized by equating the medium

with tubular urine, in direct contact with the great absorbing surface of the brush border of the proximal renal tubular epithelium. The unidirectional flux from intracellular space to extracellular space follows the pathway of reabsorbed materials into the interstitial spaces of the kidney and ultimately into the blood. Detailed observations with a variety of substrates and experimental conditions are needed before suggesting that such observations *in vitro* reflect the situation *in vivo*, but it is our belief that the scope and flexibility offered by the present analytical approach provide tools which may be helpful in understanding such complex phenomena as intestinal absorption or renal tubular reabsorption.

In contrast to our results with amino acids, FOULKES AND MILLER[21], using a similar compartmental analysis, reported that the kinetics of kidney-slice uptake of *p*-amino hippurate were explained by a series model in which all molecules traversed the extracellular space before entering the cellular compartment. One possible explanation for this apparent discrepancy lies in the very different renal tubular handling of *p*-amino hippurate and amino acids. Whereas *p*-amino hippurate is normally secreted by the tubules, and thus must move from the capillaries through the extracellular space before entering the epithelial cells, amino acids are reabsorbed from the tubule, thus obviating the need for passage through the extracellular compartment before reaching the cells.

The results with 2,4-dinitrophenol, indicating a reduction in the rate of α-aminoisobutyric acid influx as well as an acceleration of the rate of efflux, and the findings obtained during incubation studies at 27°, in which rates of influx and efflux were slowed equally, are in complete agreement with the reports of FOULKES AND MILLER[21] and COPENHAVER *et al.*[22] using *p*-amino hippurate. These observations strongly suggest that efflux phenomena—as well as influx phenomena—are metabolically linked, and are not explained solely by the laws of physical diffusion. Indeed, these and previous results[11] make it appear likely that efflux is mediated by energy-requiring sites similar to or identical with those used in influx.

In the present studies, the kinetics of incorporation of glycine and L-lysine into trichloroacetic-acid precipitable protein are of considerable interest because they do not reflect the buildup of free amino acid in the intracellular pool. HALVORSON AND GORIEN[7] and KIPNIS and co-workers[8] reported similar observations in yeast cells and diaphragm muscle, respectively. These authors suggested that functional heterogeneity of the intracellular amino acid pool could explain their findings. However, the incorporation kinetics may also be explained by postulating that external amino acids are selectively activated or incorporated into protein in or adjacent to the cell membrane without passing through the intracellular amino acid pool. In this regard, HENDLER[23] has recently presented a theoretical model for protein synthesis in intact cells in which incorporation of exogenous amino acids directly into membrane protein plays an important role. Clarification of the actual mechanisms involved must await studies in which the kinetics of incorporation of amino acids into membrane protein are separated from those characterizing synthesis of specific mitochondrial, microsomal or nuclear protein species.

It is hoped that future studies with this multi-compartment approach will lead to a clearer understanding of the mode of action of drugs, hormones and enzymes on transport phenomena in the kidney, as well as to greater insight regarding the relationship between trans-membrane movement and intracellular metabolism.

REFERENCES

1 E. F. GALE, *Bull. Johns Hopkins Hosp.*, 83 (1948) 119.
2 G. N. COHEN AND H. V. RICKENBERG, *Ann. Inst. Pasteur*, 91 (1956) 693.
3 E. HEINZ, *J. Biol. Chem.*, 211 (1954) 781.
4 E. HEINZ AND P. M. WALSH, *J. Biol. Chem.*, 233 (1958) 1488.
5 J. A. JACQUEZ, *Proc. Natl. Acad. Sci. U.S.*, 47 (1961) 153.
6 D. B. COWIE AND F. T. MCCLURE, *Biochim. Biophys. Acta*, 31 (1959) 236.
7 H. O. HALVORSON AND G. N. COHEN, *Ann. Inst. Pasteur*, 95 (1958) 73.
8 D. M. KIPNIS, E. REISS AND E. HELMREICH, *Biochim. Biophys. Acta*, 51 (1961) 519.
9 H. AKEDO AND H. N. CHRISTENSEN, *J. Biol. Chem.*, 237 (1962) 118.
10 L. E. ROSENBERG, A. BLAIR AND S. SEGAL, *Biochim. Biophys. Acta*, 54 (1961) 479.
11 L. E. ROSENBERG, S. J. DOWNING AND S. SEGAL, *J. Biol. Chem.*, 237 (1962) 2265.
12 S. SEGAL, A. BLAIR AND L. E. ROSENBERG, *Nature*, 192 (1961) 1085.
13 L. E. ROSENBERG AND S. SEGAL, *Clin. Res.*, 9 (1961) 208.
14 M. BERMAN, E. SHAHN AND M. F. WEISS, *Biophys. J.*, 2 (1962) 275.
15 M. BERMAN, M. F. WEISS AND E. SHAHN, *Biophys. J.*, 2 (1962) 289.
16 L. E. ROSENBERG, S. J. DOWNING AND S. SEGAL, *Am. J. Physiol.*, 202 (1962) 800.
17 D. STEINBERG, M. VAUGHAN, C. B. ANFINSON, J. D. GORRY AND J. LOGAN, in *Liquid Scintillation Counting*, Pergamon Press, New York, 1958, p. 230.
18 K. L. MANCHESTER AND F. G. YOUNG, *Biochem. J.*, 70 (1958) 297.
19 L. E. ROSENBERG, A. N. WEINBERG AND S. SEGAL, *Biochim. Biophys. Acta*, 48 (1961) 500.
20 J. S. ROBERTSON, *Physiol. Rev.*, 37 (1957) 133.
21 E. C. FOULKES AND B. J. MILLER, *Am. J. Physiol.*, 196 (1959) 86.
22 J. H. COPENHAVER, S. K. HONG AND R. P. FORSTER, *Federation Proc.*, 16 (1957) 25.
23 R. W HENDLER, *Nature*, 193 (1962) 821.